communications earth & environment

Article

A Nature Portfolio journal

https://doi.org/10.1038/s43247-025-02888-9

A remote input of African dust to Last Glacial Europe

Denis-Didier Rousseau[1,2,3] ✉, Catherine Chauvel[4], Peter O. Hopcroft[5], Pamela Gutiérrez[4], Ségolène Saulnier-Copard[6], Pierre Antoine[6], Markus Fuchs[7] & Alicja Ustrzycka[1]

During the Last Glacial Maximum global surface air temperatures were up to 6 °C lower than pre-industrial levels and the mineral dust cycle was highly active, with global dust loading two to four times higher than during the Holocene. Loess deposits and Greenland ice cores show peak dust concentrations during this time. While Asian sources were traditionally seen as the main contributors to dust transported to Greenland, recent studies using geochemical methods suggest a mix of Asian, North African, and European sources. Europe experienced intense dust activity, with mineral particles largely emitted from regional sources. Here we present the trace elements, and strontium and lead isotopes from Last-Glacial Maximum samples collected at 15 sites across Europe. The results reveal that fine dust originated from remote sources, potentially northern Africa. Earth System model simulations support this finding, highlighting Northern Africa's substantial role in dust deposition during glacial periods across the Northern Hemisphere.

The intensification of the dust cycle during the Last Glacial Maximum (LGM) continues to challenge our understanding of Earth's systems and aerosols. Its origin is attributed to enhanced dust emissions, but we lack constraining site-level data. Greenland ice-core records have been interpreted as recording a substantial increase in dust storms in Asian deserts[1,2]. Globally the dust emissions enhancement is attributed to i) increased atmospheric gustiness (e.g[2,3].) related to enhanced temperature gradients, ii) the generally dryer LGM (23-19 kyrs BP) climate[4], iii) reduced vegetation cover due to the low-CO_2 environment[5], and iv) the emergence of glaciogenic dust source regions[6]. In support of this, dust sediments, termed loess, that mantle vast areas of the Northern Hemisphere demonstrate that the dust cycle was even more active during the LGM in northern continents[7]. Over Europe, during the coldest phases of the last glacial period there was extensive development of loess deposits. These sediments had accumulation rates that place the area among the dustiest regions on Earth[8] and with environmental variations that are synchronous with the much larger and extremely rapid relative variations recorded over Greenland[9–11]. Geochemical data also show similarities between European loess and Greenland ice-core dust[12–16] but a posited atmospheric transport from Europe to Greenland (e.g. Schaffernicht et al.[17]) would require sporadic reversals of the westerlies. Therefore, European loess have emerged as a crucial archive for understanding the nature and climatic significance of glacial-interglacial and millennial scale dust variations over the Atlantic region.

The thickest and more complete European loess sequences, situated at 50° N latitude[11,18,19] (Fig. 1), capture abrupt warmings linked to Greenland Interstadials[20,21], marked by reduced dust and soil formation[11,18,19,22]. Cold Stadials, including the Last Glacial Maximum, that follow show high sedimentation and coarse dust, signaling a return to glacial conditions[8,18,23,24]. This pattern of alternating dust deposition and subsequent cessation is observed in marine isotope stages 3 and 2 along a longitudinal transect from France to Ukraine, with increasing grain size index, toward the Last Glacial Maximum (LGM)[18,19,24] but also a longitudinal decrease of the mass accumulation rates from western France to Ukraine during GS8 to GS3 (38.2 to 23 ka b2k). In these records the LGM stands out as a period of intensified dust emission, transport, and deposition, attributed to successive intense dust storms fueled by changes in atmospheric circulation[8,18,25]. In their study focused on the origin of dust deposited in the Greenland ice sheet, Ujvari et al.[15] compared the fine fraction of dust in ice cores with samples from potential sources, including East European loess. Their modeling-based backward trajectory analysis supported the hypothesis of a European origin for peak stadial Greenland dust, highlighting the importance of long-range transport in dust dynamics.

[1]Institute of Physics-CSE, Division of Geochronology and Environmental Isotopes, Silesian University of Technology, Gliwice, 44-100, Poland. [2]Géosciences Montpellier, Université de Montpellier, Montpellier, Cedex, 05, France. [3]Lamont Doherty Earth Observatory, Columbia University, Palisades, NY10964, USA. [4]Institut de Physique du Globe de Paris, Université Paris Cité, CNRS, F-75005 Paris, France. [5]School of Geography, Earth & Environmental Sciences, University of Birmingham, Birmingham, B15 2TT, UK. [6]Laboratoire de Géographie Physique: Environnements Quaternaires et actuels, Université Paris 1, Thiais, France. [7]Department of Geography, Justus Liebig-University Giessen, 35390 Giessen, Germany. ✉e-mail: denis-didier.rousseau@umontpellier.fr

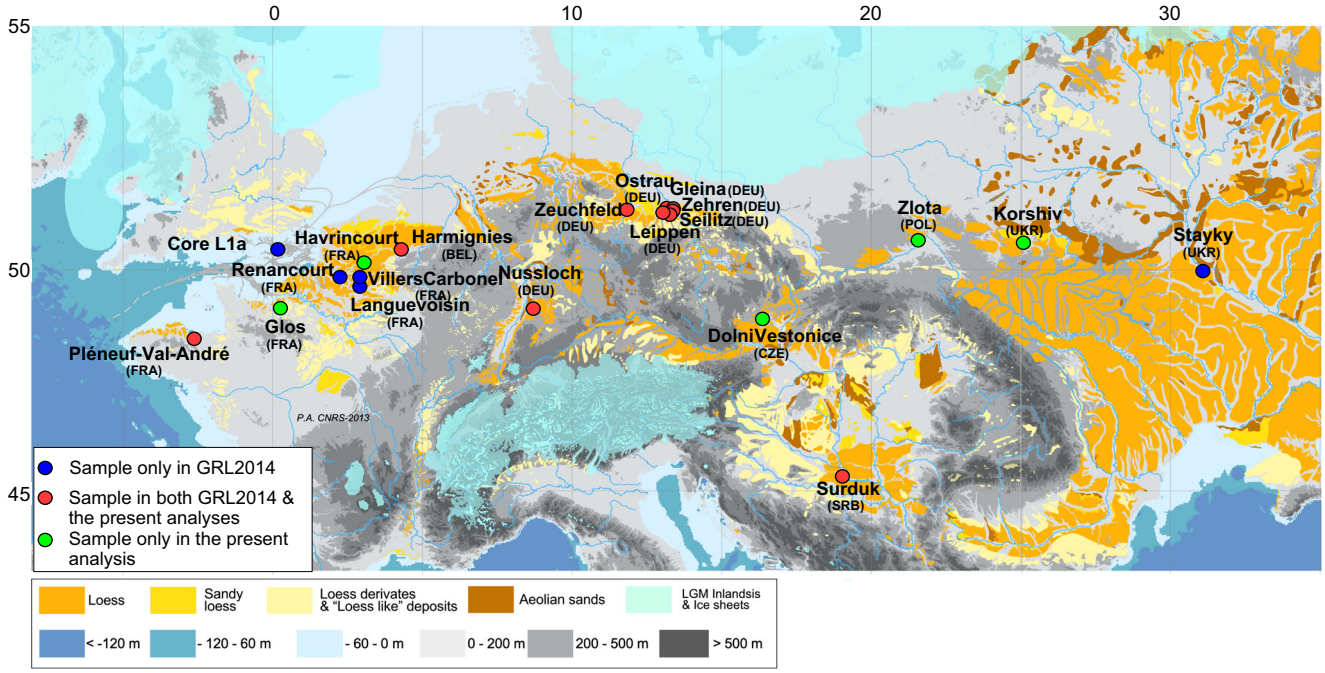

Fig. 1 | Map of European loess deposits. (after Rousseau et al.[25], modified from an original by Antoine et al.[83]). Location of the sequences analyzed. LGM Last Glacial Maximum, BEL Belgium, CZE Czech Republic, DEU Germany, FRA France, POL Poland, SBR Serbian Republic, UKR Ukraine, Core L1a from Mellett et al.[84]. The color of the bullets is given according the analysis performed on the LGM samples. The six lower icons represent topography and bathymetry.

Numerical simulations using Earth System Models have shown that changes in vegetation, influenced by millennial climate variability, modulate paleodust emission, with the dust cycle peaking in spring[26,27]. However, the three-dimensional nature of the dust field and influence of source regions further afield remain poorly constrained due to a lack of appropriate field data and integrated modeling studies.

Loess deposits in Europe provide a valuable archive for understanding past dust dynamics. A number of geochemical studies investigated these deposits in a regional context. For instance, Buggle et al.[28] and Bosq et al.[29] analyzed major and trace elements in bulk sediments and specific grain-size fractions (<32 µm and 32–100 µm), suggesting an alluvial origin from local riverbeds. Panczyk et al.[30] used U-Pb age of zircons to argue for a local to regional origin of the loess material as well as Fenn et al.[31] who combined U-Pb ages and Hf isotopes in zircons. Similar conclusions were also reached by Fenn et al.[32] who used Sr and Nd isotopes and focused on bulk and fine fractions of samples from four loess sequences along the Danube in Eastern Europe. Contrasting conclusions were reached by Stuut et al.[33] and Varga et al.[34], who suggested that coarse and fine dust fractions had different origins. However, their conclusions were primarily based on analogies with modern dust falls over Europe and coming from Northern Africa and they lacked geochemical support. In addition, none of these studies were constrained by Earth System modelling, limiting their capacity to determine the broader atmospheric transport dynamics involved.

Our previous geochemical analyses of LGM-dated loess samples along a transect near 50° N (Fig. 1) demonstrated that the dust contributors in the 48°N to 52°N range contained a lot of zircons suggesting a regional, low-altitude dust transport[25], with material originating from the nearby European regions. The high zirconium concentrations in European loess deposits suggest an overabundance of zircon, a heavy mineral indicative of low transport and local source but because zircon is mainly present in the coarse fraction of the material, it does not mean that all particle sizes are local. Indeed, fine particles can travel long distances and at higher altitudes than coarse ones. Given the incredibly dusty conditions recorded in Europe and Greenland during the LGM, and the relative proximity to the Sahara, today's largest source of dust, the study of particle-size-dependent transport dynamics is essential.

In this study, we present new geochemical and isotopic analyses of the different particle-size fractions from European loess deposits. These are coupled with Earth System Model simulations of the paleo-dust cycle to better constrain the geographic origins and transport pathways of dust during this period.

We selected three grain-size classes: 1) < 2 µm, 2) 2–20 µm, and 3) bulk; the two fine fractions are also represented in Earth System models and the bulks link our results to our previous study[25]. This size-resolved geochemical analysis (trace element and Sr and Pb isotope ratios) should enable the identification of potentially non-local sources of paleodust. These sources can be characterized by modeling of the emission, transport, and deposition of dust in Europe during the LGM time period (HadGEM2-ES[35,36],) and comparing the results with data published for various potential source regions.

Results

Geochemical results

Trace elements were measured on the three fractions mentioned above (Supplementary data file). Figure 2 shows all the results for the three fractions of the studied samples. New bulk measurements are similar to those already published[25] (Fig. 2c). The 2–20 µm fractions (Fig. 2b) have trace element patterns that resemble strongly the bulk sediments with positive zirconium (Zr) and hafnium (Hf) anomalies and negative strontium (Sr), lithium (Li) and lead (Pb) anomalies (Fig. 2b, c). By contrast, the <2 µm fractions display elevated values in Li and Pb, and low contents in Hf, Zr, and Sr (see Fig. 2a). This indicates that distinct mineralogy characterizes the three grain-size fractions, with the <2 µm particles being depleted in zircons while both the 2–20 µm fraction and the bulk sediment (which is dominated by these larger particles) are enriched in this mineral.

Figure 3 shows the variations of $^{208}Pb/^{204}Pb$ versus $^{87}Sr/^{86}Sr$ for all analyzed grain size fractions of the loess samples, including previously published bulk values[25]. First, the latest bulk measurements match well the previous observations, supporting the interpretation of a regional origin of the deposited material after transport over relatively short distances of around 1 km to 100 km maximum. In particular, the composition of bulk samples from Czech Republic and Serbia that are different from other

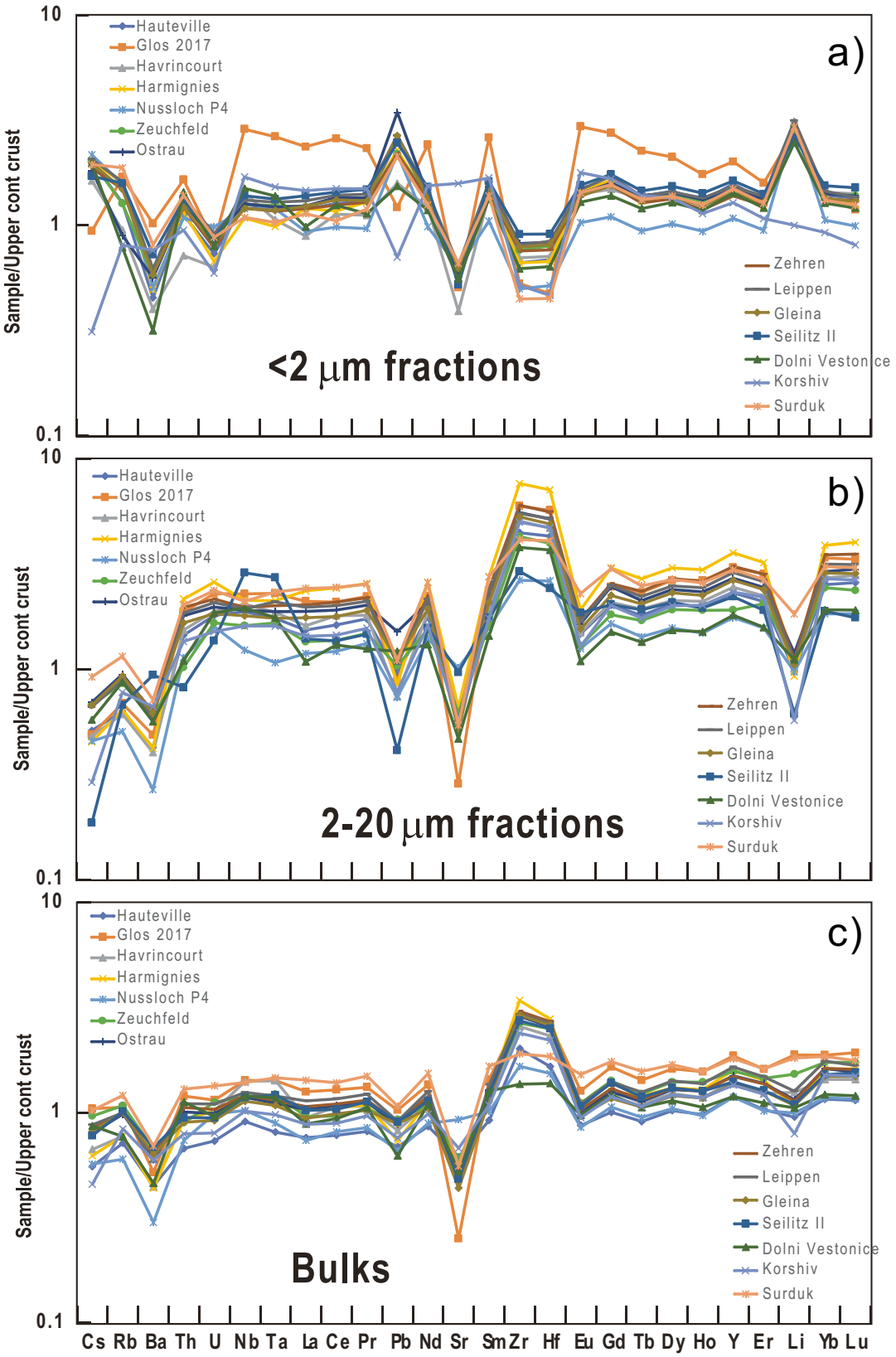

Fig. 2 | Trace element data for different grains-size fractions normalized to the average concentrations of the upper continental crust[85]**. a** < 2 μm fractions, **b** 2–20 μm fractions and **c** bulk sediments. Most sediments show similar patterns according to the respective size fractions although proportions vary greatly from site to site. Clear differences exist between the 2–20 μm size fractions with positive Hf and Zr anomalies and the <2 μm fractions with negative anomalies in Sr, Zr, and Hf. The differences are due to different mineralogy in the two fractions.

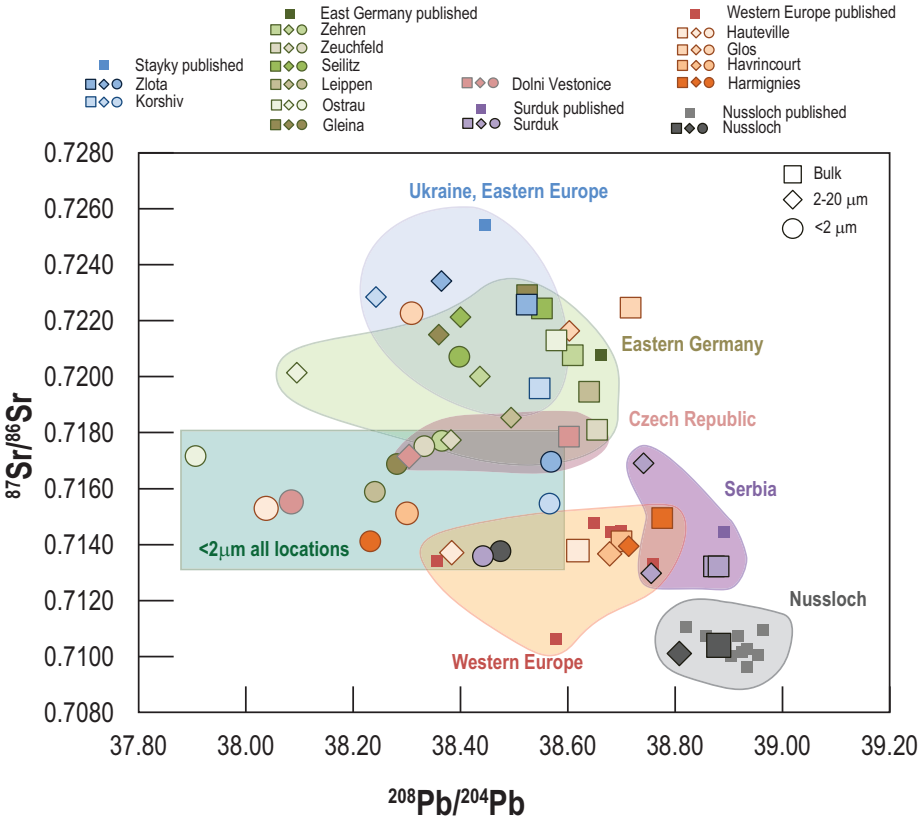

Fig. 3 | Isotope ratios of $^{87}Sr/^{86}Sr$ and $^{208}Pb/^{204}Pb$. Errors on the measurements are smaller than the symbols. Small squares represent the bulk analyses published in Rousseau et al.[25] while large symbols correspond to our latest measurements. The geographical groups are identical to those identified in Rousseau et al.[25]. The Nussloch samples are shown separately from Western Europe as they correspond to both LGM and previous and later samples.

samples, supports the original regional hypothesis[25,32] (Fig. 3). Data acquired on the 2–20 µm size fractions generally plot close to their related bulk samples but with usually lower $^{208}Pb/^{204}Pb$. This indicates that the 2–20 µm size fraction has an origin comparable to that of the bulk and that it dominates the Sr and Pb isotopic compositions. In noteworthy contrast, the <2 µm fractions have Sr and Pb isotopic compositions merging at intermediate $^{87}Sr/^{86}Sr$ and low $^{208}Pb/^{204}Pb$, in a range unrelated to those defined by the bulks or 2–20 µm data. While most <2 µm fractions have $^{87}Sr/^{86}Sr$ between 0.714 and 0.718, two exceptions exist with values > 0.720. These two samples (Glos and Seilitz) were located close to the ice wedges (see details in Lautridou[37] and Meszner et al.[38]) and contain desiccation cracks that could have been filled later on by material with a different origin. Even though the data points are shown in Fig. 3, they are omitted from the interpretation. Figure 3 demonstrates that the $^{208}Pb/^{204}Pb$ ratio of the fine fractions is systematically less radiogenic than those of the 2–20 µm fraction and the bulk rock, a feature that can easily be explained by a lack of heavy minerals such as zircon and monazite and the predominance of K-feldspar and clay in the fine fraction. Indeed, zircon and monazite being very rich in uranium and thorium, their Pb isotopic composition is usually very radiogenic with elevated $^{207}Pb/^{204}Pb$ and $^{208}Pb/^{204}Pb$ (see details in Garçon et al.[39]); they control the Pb isotopic budget of the Zr-rich coarse fractions but not that of the Zr-poor fine fractions whose Pb isotopic budget is controlled by K-feldspar and clay Garçon et al.[39]. However, the lack of clear correlation between $^{208}Pb/^{204}Pb$ and Th/Pb ratios (see Supplementary Fig. 4) demonstrates that mineral sorting is not the only cause for the changing $^{208}Pb/^{204}Pb$ (^{232}Th decays into ^{208}Pb). Some independent process is necessary and it could be dust coming from another area. Fig. 3 also shows that $^{87}Sr/^{86}Sr$ does not necessarily increase from coarse to fine fractions as should be the case considering the overwhelming presence of clay and K-feldspar in the fine fractions (see details in Garçon et al.[39]). While the <2 µm fractions of the western European loess have, as expected, slightly more radiogenic Sr isotopes than the coarser fractions, it is not the case of the eastern European loess whose <2 µm fractions are less radiogenic than the coarser fractions (see Fig. 3). In practice, all fine fractions converge to intermediate $^{87}Sr/^{86}Sr$ values no matter what the bulk and 2–20 µm values are. A first but very unlikely explanation for the low Sr isotopes of the <2 µm eastern European loess fractions could be that their fine fractions are exclusively composed of fine dust coming from the western part of Europe and that their own clay fractions have been totally blown away to the East. An alternative scenario would be that the fine fractions are not the result of mineral sorting but represent mixtures of dust from the entire area. Such scenario seems quite unrealistic given (a) the difference in trace element patterns between fine and coarse fractions that demonstrates that the fine fractions cannot be produced by grinding up coarser material (see Fig. 2) and (b) the systematically lower $^{208}Pb/^{204}Pb$ of the fine fractions relative to the coarse ones and the bulks, a feature that cannot be explained by simple mixing. We favor a different interpretation and suggest that the coupled Sr-Pb isotopic difference between fine and coarse fractions indicates that mineral phases present in the fine and coarse fractions have different origins.

The marked isotopic difference between fine-grain and coarser-grain fractions suggests different transport and different geographic sources, the source of the fine-grain fraction being substantially more uniform than that of the coarser fractions. The distinction between <2 µm and 2–20 µm—bulk fractions is important to note, given that the fine fraction represents 20 wt.% of the sediment, while the coarser fractions account for the remaining 80 wt.% (Supplementary Table 2). However, whilst the <2 µm fraction appears relatively homogenous for $^{87}Sr/^{86}Sr$ and Pb isotopes, it is not yet clear whether it represents a single source or a mixture of materials coming from several areas.

Modeling results

The inclusion of glaciogenic sources in the LGM Earth System model (ESM) simulation introduce considerable additional dust deposition over Europe (see Methods and Figs. 4, 5). This global ESM LGM simulation produces a zone of dust deposition varying up to 301 g/m^2/y over the area of this study (20W-30E by 47.5–52.5 N) for the 3.16–31.6 µm particle sizes with a zonal

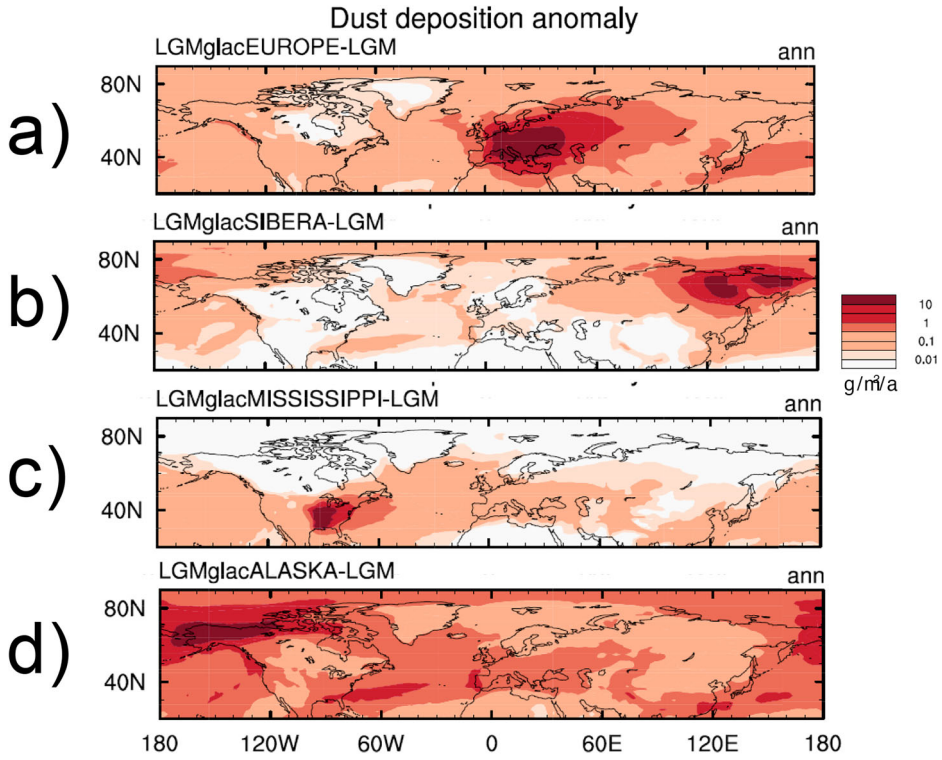

Fig. 4 | Change in LGMglac total dust deposition between simulations with glaciogenic sources active in individual regions only versus simulations with no glaciogenic sources. The active glaciogenic regions are **a** Europe, **b** Siberia, **c** Mississippi and **d** Alaska. (from Hopcroft et al.[40]). LGMglac: Last Glacial Maximum plus glaciogenic source regions following Albani et al.[57].

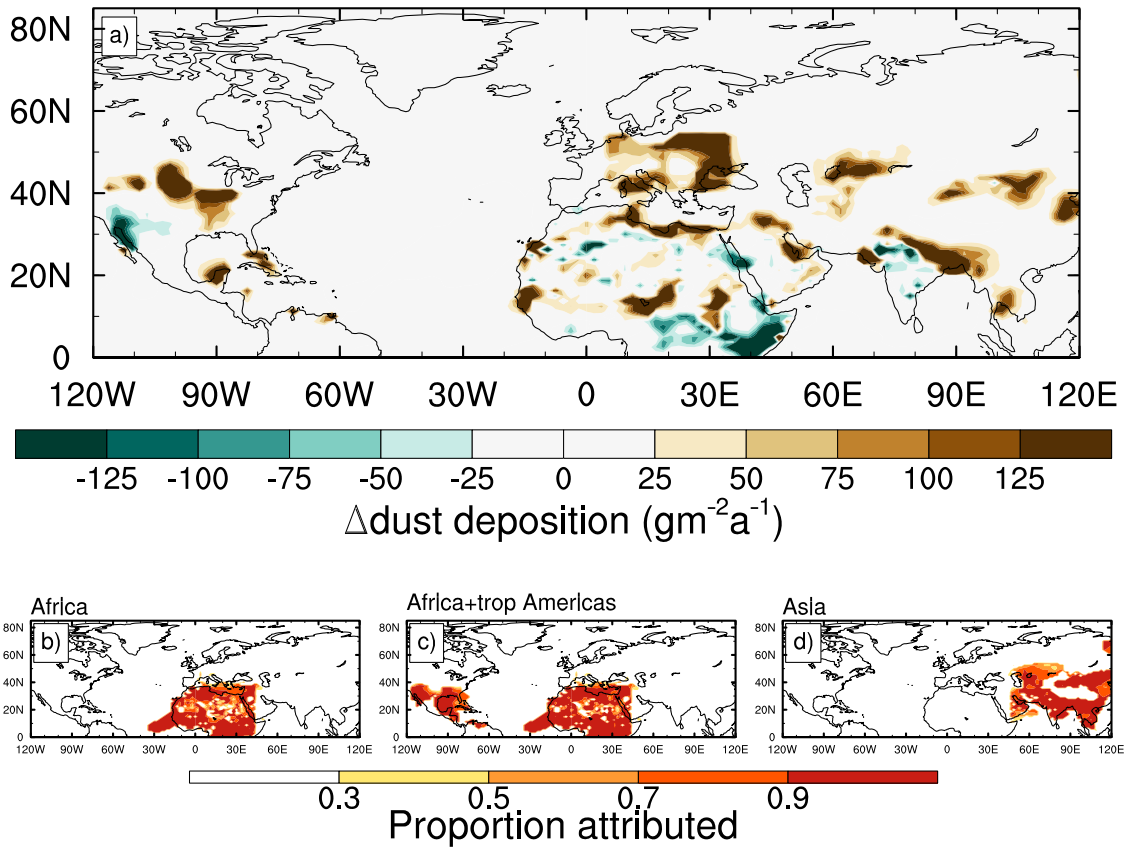

Fig. 5 | Dust deposition anomalies (LGMglac - pre-industrial) in Northern Hemisphere for the coarser particles (>3.16 μm). a Dust deposition in g m^{-2} yr^{-1} with contribution of three different sources, and contributions of different sources: **b**) Africa, **c**) Africa + tropical Americas, and **d**) Asia. LGMglac: Last Glacial Maximum plus glaciogenic source regions following Albani et al.[57].

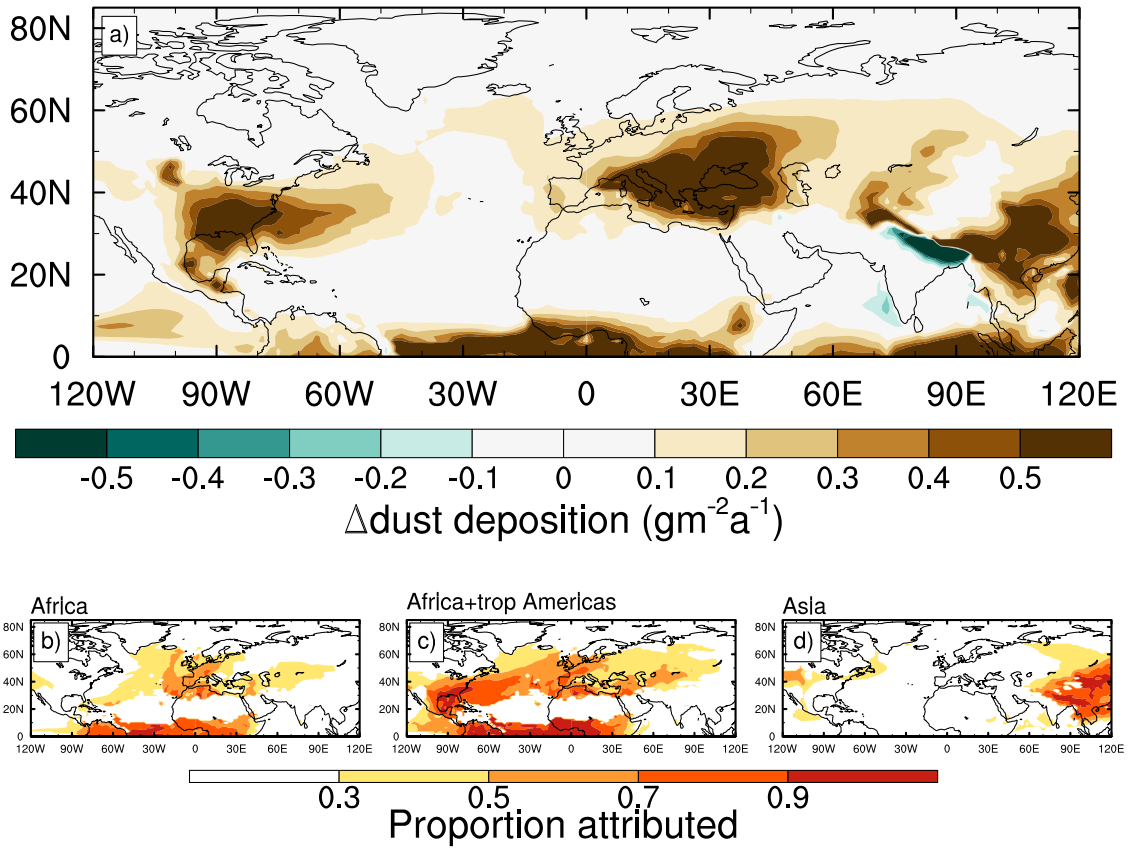

Fig. 6 | Dust deposition anomalies (LGMglac - pre-industrial) in Northern Hemisphere for the finest particles (<0.316 µm). a Dust deposition in g m^{-2} yr^{-1} with combined contribution of three different sources; individual contributions of these sources: **b** Africa, **c** Africa + tropical Americas, and **d** Asia. LGMglac: Last Glacial Maximum plus glaciogenic source regions following Albani et al.[57].

average at this latitude of 67 g/m^2/y. Over the studied transect of the European loess belt also at 50°N (Fig. 1) estimates by Rousseau et al.[8] of the LGM mass accumulation rates, (taking into account the paleosol development in their age models), give values of 406 to 623 g/m^2/y for the grain size fraction 4.6–26 µm between 38.2 to 23 b2k (see Supplementary File 1 and Fig. 4 in ref. 8). Although Fig. 6 shows substantial deposition of fine particles further southwards of main loess belt areas, the total dust flux is greatest to the north and eastern areas of Europe (see Fig. 5) where local glaciogenic source regions have been prescribed in the model. The inclusion of freshwater forcing in the model, which cools the Atlantic is simulated in the LGMglac +fw1 simulation. This shows a substantially increased mean dust flux at 50°N of 122 g/m^2/y which is driven by increased emissions from the Sahel and elsewhere and reduced wet deposition. Both of these features are partly driven by the southward shift of the intertropical convergence zone[40].

Sensitivity simulations show that the additional dust deposited over the European landmass is sourced from three main regions (Fig. 6, See Methods). The larger particle fraction (here particles >3.16 µm) is completely dominated by locally emitted particles with only around 1% coming from Africa and even less from elsewhere (Supplementary Table 3). This is to be expected given the rapid gravitational settling and limited transport range of these larger particles which is exacerbated by a common deficiency across ESMs that sees these particles settling too rapidly (e.g. Ratcliffe et al.[41]). We evaluate the potential of a remote sources using the sum of the two smaller size bins in the model (<0.316 µm). This should allow a clear separation from the mostly local dust mobilization simulated for the heavier particles. This analysis (Supplementary Table 3) shows for the LGMglac simulation a significant proportion is derived from Africa (43%) and the tropical Americas (12%), with only 11% derived from Asia.

The glaciogenic flux is dominated by emissions from within Europe itself and from North America, including Alaska (e.g. Fig. 4). A major component of the fine particle dust flux in Europe is therefore remotely sourced in this simulation and 55% of this is derived from the land-masses surrounding the tropical (35°S-35°N) Atlantic, including Africa. The LGMglac+fw1 simulation shows similar contributions but with a slightly larger component from Asia (see Supplementary Table 3). It can be concluded that both the LGMglac and LGMglac+fw1 simulations provide evidence to support the hypothesis that the fine grain dust identified through the geochemical data originated from a remote source. Furthermore, both simulations point to Africa as a major contributor to this source influx.

Discussion

Potential remote sources and transport patterns

The <2 µm fractions from European loess samples define a horizontal band in the $^{87}Sr/^{86}Sr$ vs $^{208}Pb/^{204}Pb$ isotopic space (Fig. 3) and it can be noticed that the $^{208}Pb/^{204}Pb$ ratio generally increases with longitude. Indeed, a statistically significant increase from Brittany to Ukraine occurs for the Pb isotopic ratio of the <2 µm fraction, while no such relationship exists for the 2-20 µm fraction (Supplementary Fig. 2), indicating that the overall composition of the fine material is disconnected from the local sources recorded by the coarser fraction and the bulk. The geographical change in $^{208}Pb/^{204}Pb$ of the fine fraction (37.9 to 38.6 units) and the rather constant $^{87}Sr/^{86}Sr$ ratio at ≈0.716 reflect therefore a source that is independent of the regional geology. A comparison of the fractions from European samples with data from the available literature for other areas in $^{87}Sr/^{86}Sr$ versus $^{208}Pb/^{204}Pb$ isotopic space helps us figure out the long-distance origin (see Fig. 7). This

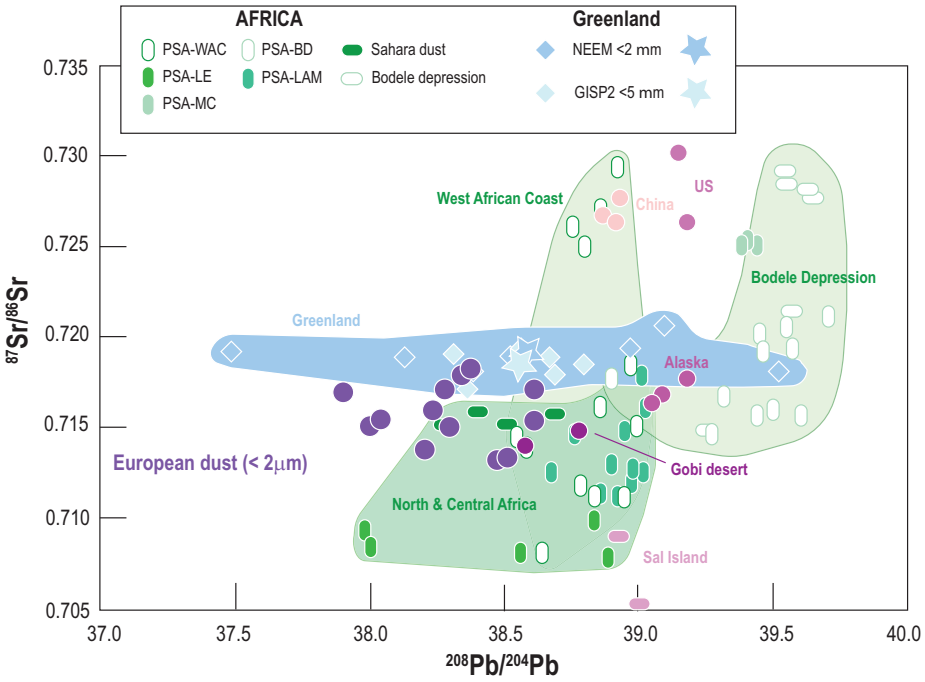

Fig. 7 | Comparison of <2 m fractions from European samples with data from the literature for other areas in $^{87}Sr/^{86}Sr$ versus $^{208}Pb/^{204}Pb$ isotopic space. Other samples include LGM samples from <5 μm fractions for US, Chinese and Alaskan loess samples, GISP2 < 5 μm dust samples (from Biscaye et al.[42]; Svensson et al.[45]) and NEEM Greenland ice core <2 μm dust from Huan et al.[14] (the averages are shown with stars). Modern <5 μm dust samples from Gobi desert are from Biscaye et al.[42] while Sahara dust samples, Bodele Depression and Sal Island surface sediment samples are from Abouchami et al.[43]. Northern African soil samples assigned to different PSA are from Guisoveau et al.[44].

comparison excludes US, Chinese, and Alaskan loess samples (less than 5 μm fractions) and Gobi desert samples (less than 5 μm from Biscaye et al.[42].) as potential sources. By contrast, similarities appear with the Bodele and North African samples[43]. Indeed, dust collected at various longitudes in Africa define a similar range of $^{208}Pb/^{204}Pb$ with lower and more variable ratios on the northern side of the Sahara than in the Bodele depression and the southern part of the Sahara (see Fig. 7). For Sr isotopes, the direct comparison between potential sources and the fine fraction of the European loess is more difficult to evaluate due to the removal of carbonates for most published data, a procedure that we did not use in this study and that affects the reported $^{87}Sr/^{86}Sr$. It remains that the northern part of Sahara produce dust whose Sr isotopes are compatible with the values measured here for the <2 μm fraction of the European loess. Here we suggest that such source could be northern Africa.

To further explore the African hypothesis, we also examine lead isotope ratios from five North African potential sources areas (PSA) as defined by Guinoiseau et al.[44]: Libya-Algeria-Mali (PSA_{LAM}), Libya-Egypt (PSA_{LE}), Bodélé Depression (PSA_{BD}), Mali Center (PSA_{MC}) and West African Coast (PSA_{WAC}). Compared to the data generated for Europe, there is a close relationship between the Pb isotopic ratios in the soil samples collected in various parts of Northern Africa (PSA_{LE}, some PSA_{WAC} and the Sahara dust), and our <2 μm fractions of loess samples. Two samples of the North African dust storms that reached Europe in 2024, collected in Grenoble (French Alps), also plot among the North African samples (see Fig. 8a and b). This supports the hypothesis of a sub-tropical Northern African origin of the fine material in the European loess samples. The identification and characterization of this long-range transport over Europe for the <2 μm fraction is of particular importance, as it represents a non-negligible weight fraction of all the European loess samples (Supplementary Table 2).

The composition of the fine fraction of the European loess can be further compared to the fine dust deposited in the Greenland GISP2 ice-core. In their studies, both Biscaye et al.[42] and Svensson et al.[45] concluded that the main source of the fine dust deposited on top of the Greenland ice-sheet was from both Gobi and Taklimakan deserts. Our first-hand data on the fine fraction of the European loess provide some original insight for the potential source of dust in Greenland during the Last Glacial Maximum. Figure 7 shows that both GISP2 and NEEM data fall in the same field as several of our recently acquired data on the fine loess fraction suggesting that the source of dust in Greenland could well be meaningfully influenced by the dust deposited in Europe during the same time period. Data reported more recently by Han et al.[14] for samples from the NEEM Greenland ice-core, covering the interval from 30,800 years BP to 8,260 years BP, define a very large range of $^{208}Pb/^{204}Pb$ but they still overlap with the GISP2 < 5 μm samples and the <2 μm fractions of European loess in Fig. 7. Finally, Fig. 7 shows that a potential mix of African and Asian origins for the <2 μm in European loess deposits is possible.

Transport of dust from the Sahara to the Arctic has also been observed sporadically over Iceland[46]. Over a 12-year period, fifteen Saharan dust events were identified, indicating a southerly circulation that allowed particles as large as 100 μm to reach such latitudes. Recently, several dust storms also reached mainland Europe in March and June 2024 and the Pb isotope ratios indicate a Saharan origin (see Fig. 8). Israelevich et al.[47] have also documented a satellite observed aerosol optical thickness (AOT) over the period 2001-2010 that depicts two main routes for Saharan dust reaching Europe[47]. In Western Europe (15°W–5°E), dust is transported westward by spring trade winds, subsequently turning north over the Atlantic Ocean, and finally shifting eastwards. In addition, they described a synchronous increase in aerosol optical thickness over the southern slopes of the Alps and the Pyrenees. In Central and Eastern Europe (5°E–40°E), Saharan dust is transported northward by air masses crossing the Mediterranean. These modern observations of the long-distance transport of Saharan dust, with their emphasis on the Atlantic route enabling subtropical particles to reach Europe, as well as the high northern latitudes, demonstrate direct atmospheric evidence of Saharan dust reaching Europe.

In our simulations the greatest dust deposition fluxes over Europe occur in Northern Hemisphere spring months (MAM) across different time periods. The increased influx of dust from Africa is dominated by changes in transport rather than emissions because the total emissions over North Africa are comparable in the pre-industrial and LGM simulations, for example. During the 20% of months with the highest dust deposition fluxes over Europe in the pre-industrial simulation, the circulation anomalies resemble a North Atlantic ridging pattern which is known to bring dust to Europe today (e.g. Cuevas-Agullo et al.[48]). In the dustiest 20% of months of the LGM simulations (with or without glaciogenic dust sources) a tripole anomaly of geopotential height (at 500 mbar) develops between Greenland and North Africa (as shown in Fig. 9) with a band of low geopotential height

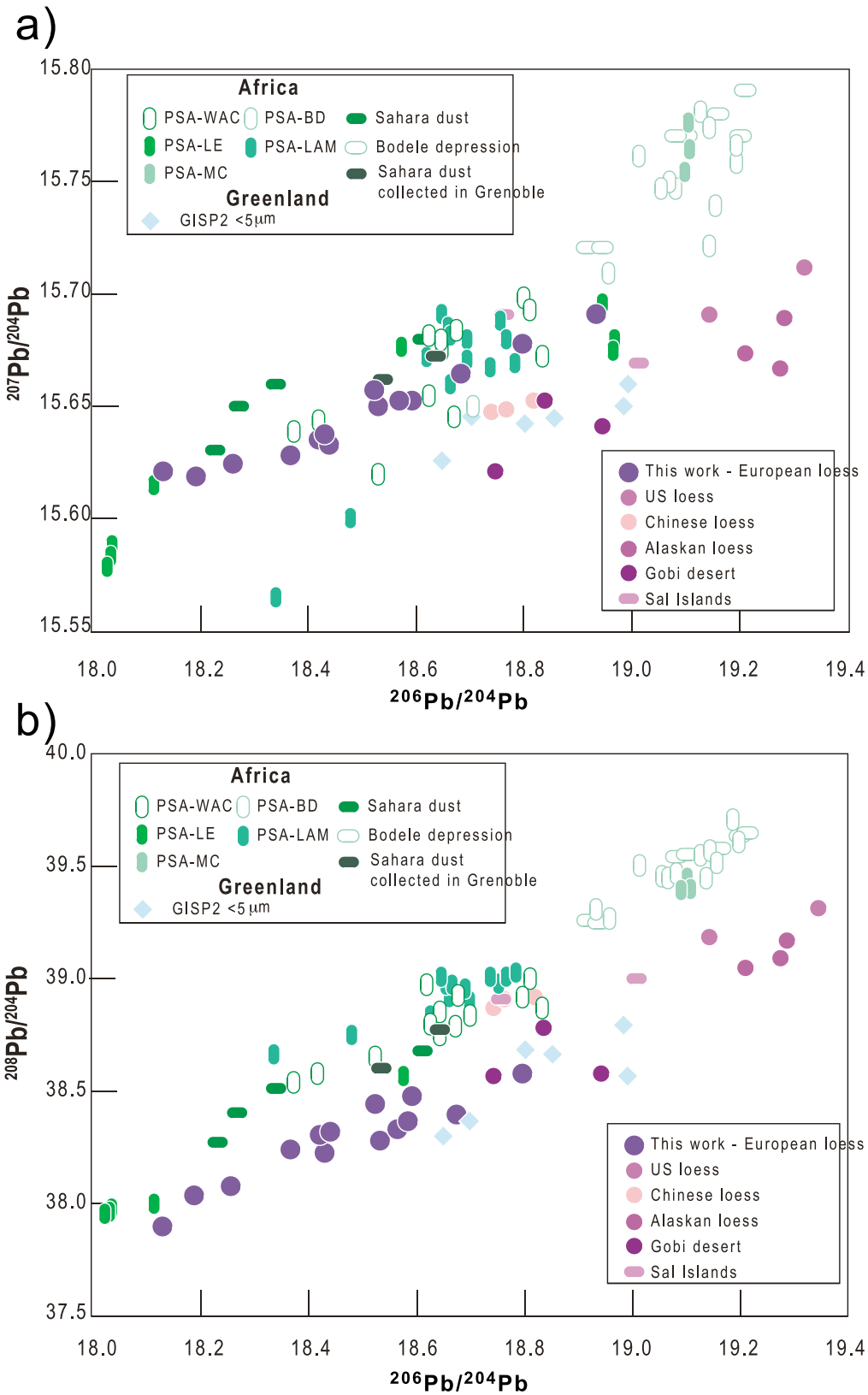

Fig. 8 | Plot of lead isotope ratios. The fine fraction of European loess is compared to the <5 μm fractions of samples from various sites: US, Chinese and Alaskan loess, Gobi desert and GISP2 samples[42]. Samples from 2024 dust storms reaching Europe, Grenoble, and collected by one of us are also indicated. Samples from Saharan dust, Bodele depression, Sal Islands[43] and Saharan and Sahelian potential source area samples[44] are also shown. **a** $^{207}Pb/^{204}Pb$ versus $^{206}Pb/^{204}Pb$ and **b** $^{208}Pb/^{204}Pb$ versus $^{206}Pb/^{204}Pb$.

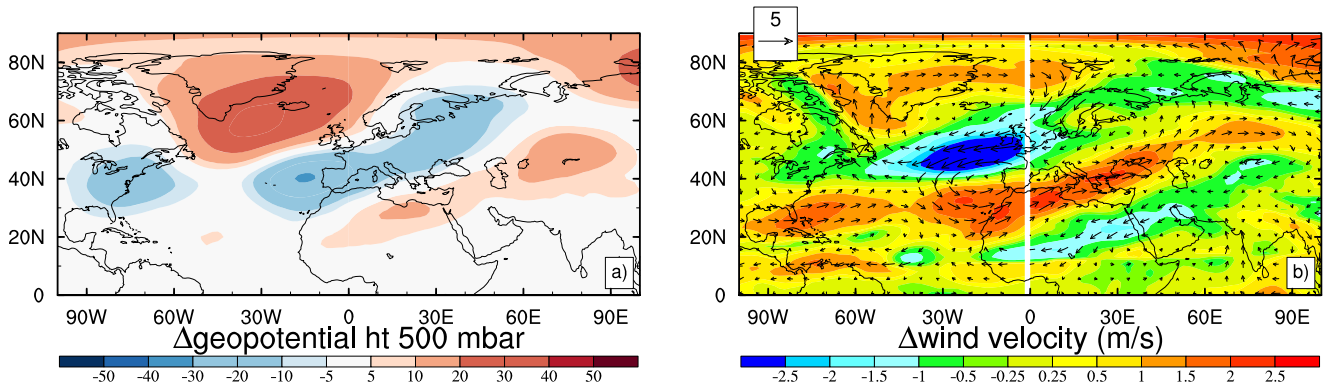

Fig. 9 | Anomalies calculated from monthly-means exceeding the 80th percentile for dust flux over Europe (for the finest two dust size bins) minus remaining months for the LGM simulation for Spring (MAM) for. a) the 500 mbar geopotential height (m) and **b)** the wind velocity (shading) and vectors (arrows) in ms^{-1}.

anomalies between two areas of positive anomalies (over Greenland and North Africa). This tripole effectively forces anticyclonic wind anomalies that are orientated from the North West of the Sahara, creating an efficient transport pathway for dust towards Europe. This LGM geopotential height anomaly (Fig. 9) has previously been associated with the most extreme southerly position of the North Atlantic sub-tropical jet position in glacial climates (e.g. Merz et al.[49]) and this southwards shift is also evident in HadGEM2. During these phases the jet position which is already further south than in the pre-industrial can therefore even more readily interact with air masses containing dust from the Sahara. The mean-state LGM southwards shift of the jet stream is associated with both topographic and cooling effects of the LGM boundary conditions (e.g. Merz et al.[49]; Roberts et al.[50]) and appears to be relatively robust across models (e.g. Wang et al.[51]). Although beyond the scope of this work, further model analyses would clarify the relative contributions of these different synoptic conditions on dust variability (e.g. Schaffernicht et al.[17]).

Broader implications

Current dust deposition rates in Europe averaged annually for PM10 (<10 μm), vary between 1–10 $g\,m^{-2}\,yr^{-1}$ [52], whilst the European mass accumulation rate for the LGM is up to 66–181 $g\,m^{-2}\,yr^{-1}$ for the <10 μm fraction[8] highlighting the magnitude of the differences between the two time periods. The significance of such dust variation in past climates on decadal to millennial scales has been often overlooked due to a series of uncertainties. These include the quantification, transport, chronology, radiative effects, and data-model comparisons of (paleo)dust. Indeed, despite the advances in satellite observations and modelling, the IPCC AR6 report[53] draws attention to the persistent high uncertainties in predicting modern dust cycles and feedbacks, which are even greater for past climates such as the Last Climate Cycle (LCC -130-12 ka BP). Rapid climate events in the LCC saw susbtantial dust variations, as measured in Greenland ice cores records covering the Greenland stadial-interstadial cycles. Additional complications arise because the radiative effects of fine and coarse particles are generally opposite[54,55] and larger particles are observed to be more long-lived than based on theoretical considerations alone (e.g. Ratcliffe et al.[41]).

Our latest geochemical analyses of LGM samples indicate that the coarser fractions (2–20 μm and bulk) derive from local sources, as previously described[15,25,32], while the finer dust fraction (<2 μm), with its rather homogeneous Sr-Pb composition, originates from a more distant source that we interpreted as being Northern Africa. This interpretation would indicate that the finer deposited material in Europe may have been transported at time intervals, as it occurs in modern time, or even at a different season than the coarser particles estimated to be mobilized at the end of winter until beginning of Spring[26]. Our suggestion is that coarse material was emitted, transported at low elevation and deposited locally/regionally. In contrast, the fine material deposited in European loess belt was at least partly sourced remotely and for this, the dust must have been transported at a higher elevation most likely from Africa, transport that is supported by our model simulations. A recent study of an Alpine ice core shows changes in dust and sea salt during the last ice age. It found high levels of sea salt and calcium, likely caused by stronger winds and more dust from the Sahara[56]. These results match what we found in our own research. The average values of the Sr and Pb isotopic ratios in Greenland ice cores are also very similar to the values measured in European <2 μm loess samples. This observation hints at a potential influence of this remote source over Greenland as suggested for stadial phases by Ujvari et al.[15]. This would question the paradigm that dust arriving during the glacial was predominantly sourced from Asia (e.g. see also Han et al.[14]; Ro et al.[16]).

It is known that dust exerts a noteworthy influence on the Earth's radiation budget, albeit with opposing effects in the short- and long-wave spectra (e.g. Kok et al.[55]). This has long been thought to have been amplified during the LGM (e.g. Albani et al.[57]). However, models have been partly contingent on contemporary dust size distributions, which may not accurately reflect the radiative impacts of the past[58] and have had relatively little size-resolved empirical data for validation. A remote input of fine particle dust to Europe implies a particular radiative forcing effect that was in operation during the LGM but a full characterization would require innovative atmospheric simulations with radiative forcing diagnostics and constrained particle size distributions which is beyond the scope of the present study. We can postulate that the abrupt shifts between Greenland stadials and interstadials during Dansgaard-Oeschger cycles of the last glacial period may have impacted this remote transport pathway and therefore altered regional dust radiative forcing quite substantially. As a consequence, despite this apparent importance of dust in past climate dynamics, its impact on rapid climate changes calls for further study.

Conclusions

Our results demonstrate, for the first time, that both local and remote transport pathways prevailed during the deposition of LGM paleodust over Europe. At low elevation coarse material is transported over relative short distances regionally via westerlies, in agreement with the observed wind directions and loess landforms described from western Europe[59,60], in the Rhine valley[61] and eastern Europe[62,63] (see Supplementary Fig. 3). Conversely the fine (<2 μm) grain size fraction of the dust material has a different geochemical signature, and the observed apparent homogeneity thus suggests a long-distance transport either dominated by a single remote source or by a relative constant combination of remote sources.

We therefore propose that transport from Northern Africa to Europe was sizable and larger than previously thought during the LGM. Our combination of size-resolved geochemical analyses with state-of-the-art modeling is a promising avenue for reconstructing the complex 3D structure of dust during the LGM and this will engender better understanding of dust's radiative forcing and biogeochemical interactions.

Materials and methods

Material

Loess samples (Supplementary Table 1) of about 200 g have been prepared at LGP Thiais to extract the studied grain size fractions. Particle size separations were carried out on at least 10 g of dry sample. First, the entire sample was sieved with demineralized water on 63 µm and 20 µm sieves. The rejects were recovered, dried and weighed. The clay fraction was obtained by decanting the fraction below 20 µm. The rest of the sample was mixed and left to settle for 1 h. The supernatant is then recovered. This operation is repeated until a transparent supernatant is obtained. The two fractions thus obtained are dried and weighed. The size (diameter) of the different fractions was then checked by laser granulometry. Supplementary Table 2 show the proportion of the four grain size fractions separated from the LGM loess sediments.

Methods

The particle size fractions of the samples were crushed, and trace element concentrations, as well as Sr and Pb isotopes (Supplementary data file), were measured following the protocol of Chauvel et al.[64]. The analysis of lead and strontium are conducted on sediment powder without leaching to avoid preferential dissolution of mineral phases that could be rich in Pb (see Supplementary Fig. 4). Chemical separations and isotopic analyses are carried out at IPGP using the same protocol as described in Rousseau et al.[25].

We analyze a suite of Last Glacial Maximum (LGM) simulations performed with the Earth System model HadGEM2-ES[35,36]. This model has a horizontal resolution of 1.875° × 1.25° (longitude-latitude) with 38 unequally spaced vertical levels that reach into the lower stratosphere[35]. HadGEM2-ES has been widely used in the Couple Model Intercomparison Project 5 (CMIP5) and to study past[65,66], present[67], and future climate[68]. HadGEM2-ES includes an interactive mineral dust cycle that is directly coupled to the atmosphere and dynamic vegetation[69,70]. Dust is represented with six size classes with bin boundaries at 0.0316, 0.1, 0.316, 1.0, 3.16, 10.0 and 31.6 µm. Emissions are calculated every timestep as a function of bare soil fraction, soil moisture, and wind speed. Dust is then represented using six atmospheric tracers which are subject to dry and wet deposition. Neither direct dust-cloud interactions or non-spherical particles are represented. Previous studies have evaluated both the pre-industrial and present-day simulations of mineral dust with HadGEM2-ES[71–73] finding that it does a relatively good simulation.

The LGM simulation with HadGEM2 has been described before[73,74] and is forced with ice-sheet area, topography, and sea-level from ICE-5G[75], greenhouse gas concentrations from ice-core records[76–78], and Earth's orbital parameters as computed by Berger[79]. The model parameters in the land-surface required re-tuning from the release model version in order to produce a stable climate state for both the pre-industrial and the LGM[73] and we use these updated parameters in all simulations. In the LGM simulation, monthly sea-surface temperatures and sea-ice distribution were prescribed from simulations of the LGM with a slightly lower-resolution coupled atmosphere-ocean model HadCM3[80,81]. The LGM HadGEM2-ES simulation is 50 model years, with the final 30 years used for calculating climatologies. Glaciogenic dust sources were added based on Albani et al.[57] and as described before Hopcroft et al.[40]. This simulation is labelled LGMglac. Both the standard and glaciogenic LGM simulations were also run with stadial conditions by prescribing SSTs and sea-ice produced in coupled HadCM3 simulations forced with 100 years of 1.0 Sv (1 Sv = 106 m^3s^{-1}) of freshwater input over the North Atlantic. These simulations are LGM +fw1.0 and LGMglac+fw1.0, respectively[40].

All of the HadGEM2 simulations used in this work were re-run but with emissions restricted to particular regions in order to identify the source origin of the changes in dust deposited during each time period. We setup parallel simulations with emissions restricted to (i) Africa, (ii) Africa and tropical Americas (labelled *Atlantic region*), or (iii) Asia. The dust deposition is compared with the equivalent restricted-source region simulations (see Supplementary Table 3).

Reporting summary

Further information on research design is available in the Nature Portfolio Reporting Summary linked to this article.

Data availability

In addition to the new data produced in this study, we used published data listed in the references. The data that supports the findings of this study are provided in the Supplementary Tables and the Supplementary Data file. They are also available in the open access PANGAEA Data Repository[82].

Received: 31 December 2024; Accepted: 7 October 2025;
Published online: 27 October 2025

References

1. Ruth, U. et al. Ice core evidence for a very tight link between North Atlantic and east Asian glacial climate. *Geophys. Res. Lett*. **34**, L03706 (2007).
2. Schupbach, S. et al. Greenland records of aerosol source and atmospheric lifetime changes from the Eemian to the Holocene. *Nature Commun*. **9**, 1476 (2018).
3. Fuhrer, K., Wolff, E. W. & Johnsen, S. J. Timescales for dust variability in the Greenland Ice Core Project (GRIP) ice core in the last 100,000 years. *J. Geophys. Res. -Atmospheres* **104**, 31043–31052 (1999).
4. Kageyama, M. et al. The PMIP4-CMIP6 Last Glacial Maximum experiments: preliminary results and comparison with the PMIP3-CMIP5 simulations. *Clim. Past* **17**, 1065–1089 (2021).
5. Mahowald, N. et al. Dust sources and deposition during the last glacial maximum and current climate: A comparison of model results with paleodata from ice cores and marine sediments. *J. Geophys. Res.* **104**, 15895–15916 (1999).
6. Mahowald, N. et al. Change in atmospheric mineral aerosols in response to climate: Last glacial period, preindustrial, modern, and doubled carbon dioxide climates. *J. Geophys. Res.-Atmospheres* **111**, D10202 (2006).
7. Crouvi, O. et al. Loess records. in *Reference Module in Earth Systems and Environmental Sciences* (Elsevier, 2024). https://doi.org/10.1016/B978-0-323-99931-1.00273-7.
8. Rousseau, D.-D., Antoine, P. & Sun, Y. How dusty was the last glacial maximum over Europe? *Quat. Sci. Rev*. **254**, 106775 (2021).
9. Moine, O. et al. The impact of Last Glacial climate variability in west-European loess revealed by radiocarbon dating of fossil earthworm granules. *Proc. Natl. Acad. Sci. USA.* **114**, 6209–6214 (2017).
10. Újvári, G. et al. Coupled European and Greenland last glacial dust activity driven by North Atlantic climate. *Proc. Nat. Acad. Sci. USA* **114**, E10632–E10638 (2017).
11. Rousseau, D. D. et al. MIS3 & 2) millennial oscillations in Greenland dust and Eurasian aeolian records - A paleosol perspective. *Quat. Sci. Rev.* **169**, 99–113 (2017).
12. Újvári, G. et al. Evaluating the use of clay mineralogy, Sr–Nd isotopes and zircon U–Pb ages in tracking dust provenance: An example from loess of the Carpathian Basin. *Chem. Geol.* **304**, 83–96 (2012).
13. Ujvari, G. et al. Two possible source regions for central Greenland last glacial dust. *Geophys. Res. Lett*. **42**, 10399–10408 (2015).
14. Han, C. et al. High-resolution isotopic evidence for a potential Saharan provenance of Greenland glacial dust. *Sci. Rep.* **8**, 15582 (2018).
15. Újvári, G. et al. Greenland ice core record of last glacial dust sources and atmospheric circulation. *J. Geophys. Res. -Atmospheres* **127**, e2022JD036597 (2022).
16. Ro, S. et al. Millennial-scale variability of Greenland dust provenance during the last glacial maximum as determined by single particle analysis. *Sci. Rep.* **14**, 2040 (2024).
17. Schaffernicht, E. J., Ludwig, P. & Shao, Y. Linkage between dust cycle and loess of the Last Glacial Maximum in Europe. *Atmos. Chem. Phys.* **20**, 4969–4986 (2020).

18. Antoine, P. et al. Rapid and cyclic aeolian deposition during the Last Glacial in European loess: a high-resolution record from Nussloch, Germany. *Quat. Sci. Rev.* **28**, 2955–2973 (2009).
19. Rousseau, D.-D. et al. North Atlantic abrupt climatic events of the last glacial period recorded in Ukrainian loess deposits. *Clim. Past* **7**, 221–234 (2011).
20. Bond, G. et al. Evidence for massive discharges of icebergs into the North Atlantic Ocean during the last glacial period. *Nature* **360**, 245–249 (1992).
21. Johnsen, S. J. et al. Oxygen isotope and palaeotemperature records from six Greenland ice-core stations: Camp Century, Dye-3, GRIP, GISP2, Renland and NorthGRIP. *J. Quat. Sci.* **16**, 299–307 (2001).
22. Rousseau, D.-D. et al. Link between European and North Atlantic abrupt climate changes over the last glaciation. *Geophys. Res. Lett*. **34**, L22713 (2007).
23. Rousseau, D.-D. et al. Evidence of cyclic dust deposition in the US Great plains during the last deglaciation from the high-resolution analysis of the Peoria Loess in the Eustis sequence (Nebraska, USA). *Earth Planet. Sci. Lett.* **262**, 159–174 (2007).
24. Rousseau, D. D. et al. Eurasian contribution to the last glacial dust cycle: how are loess sequences built? *Clim. Past* **13**, 1181–1197 (2017).
25. Rousseau, D.-D. et al. European glacial dust deposits: Geochemical constraints on atmospheric dust cycle modeling. *Geophys. Res. Lett.* **41**, 7666–7674 (2014).
26. Sima, A. et al. Imprint of North-Atlantic abrupt climate changes on western European loess deposits as viewed in a dust emission model. *Quat. Sci. Rev.* **28**, 2851–2866 (2009).
27. Sima, A. et al. Modeling dust emission response to North Atlantic millennial-scale climate variations from the perspective of East European MIS3 loess deposits. *Clim. Past* **9**, 1385–1402 (2013).
28. Buggle, B. et al. Geochemical characterization and origin of southeastern and eastern European loesses (Serbia, Romania, Ukraine). *Quat. Sci. Rev.* **27**, 1058–1075 (2008).
29. Bosq, M., Bertran, P., Degeai, J.-P., Queffelec, A. & Moine, O. Geochemical signature of sources, recycling and weathering in the Last Glacial loess from the Rhône Valley (southeast France) and comparison with other European regions. *Aeolian Res* **42**, 100561 (2020).
30. Pańczyk, M., Nawrocki, J., Bogucki, A. B., Gozhik, P. & Łanczont, M. Possible sources and transport pathways of loess deposited in Poland and Ukraine from detrital zircon U-Pb age spectra. *Aeolian Res* **45**, 100598 (2020).
31. Fenn, K. et al. The provenance of Danubian loess. *Earth-Sci. Rev.* **226**, 103920 (2022).
32. Fenn, K., Millar, I. L., Bird, A., Veres, D. & Wagner, D. Provenance of late Pleistocene loess in central and eastern Europe: isotopic evidence for dominant local sediment sources. *Sci. Rep.* **15**, 1–15 (2025).
33. Stuut, J.-B., Smalley, I. & O'Hara-Dhand, K. Aeolian dust in Europe: African sources and European deposits. *Quat. Int.* **198**, 234–245 (2009).
34. Varga, G., Cserháti, C., Kovács, J. & Szalai, Z. Saharan dust deposition in the Carpathian Basin and its possible effects on interglacial soil formation. *Aeolian Res* **22**, 1–12 (2016).
35. Martin, G. et al. The HadGEM2 family of Met Office Unified Model climate configurations. *Geosci. Model. Dev.* **4**, 723–757 (2011).
36. Collins, W. et al. Development and evaluation of an Earth-System model-HadGEM2. *Geosci. Model. Dev.* **4**, 1051–1075 (2011).
37. Lautridou, J.-P. Le cycle périglaciaire pléistocène en Europe du Nord-Ouest et plus particulièrement en Normandie. (Université de Caen, Centre de Géomorphologie, 1985).
38. Meszner, S., Fuchs, M. & Faust, D. Loess-Palaeosol-Sequences from the loess area of Saxony (Germany). *EQ Quat. Sci. J.* **60**, 4 (2011).
39. Garçon, M., Chauvel, C., France-Lanord, C., Limonta, M. & Garzanti, E. Which minerals control the Nd–Hf–Sr–Pb isotopic compositions of river sediments?. *Chem. Geol.* **364**, 42–55 (2014).
40. Hopcroft, P. O., Pichat, S., Valdes, P. J. & Kienast, S. S. Sensitivity of the tropical dust cycle to glacial abrupt climate changes. *Geophys. Res. Lett.* **50**, e2022GL101197 (2023).
41. Ratcliffe, N. G. et al. Long range transport of coarse mineral dust: an evaluation of the Met Office Unified Model against aircraft observations. *Atmos. Chem. Phys.* **24**, 12161–12181 (2024).
42. Biscaye, P. E. et al. Asian provenance of glacial dust (Stage 2) in the GISP2 ice core, summit, Greenland. *J. Geophys. Res.* **102**, 26,765–26,781 (1997).
43. Abouchami, W. et al. Geochemical and isotopic characterization of the Bodélé Depression dust source and implications for transatlantic dust transport to the Amazon Basin. *Earth Planet. Sci. Lett.* **380**, 112–123 (2013).
44. Guinoiseau, D. et al. Characterization of Saharan and Sahelian dust sources based on geochemical and radiogenic isotope signatures. *Quat. Sci. Rev.* **293**, 107729 (2022).
45. Svensson, A., Biscaye, P. E. & Grousset, F. E. Characterization of late glacial continental dust in the Greenland Ice Core Project ice core. *J. Geophys. Res. -Atmospheres* **105**, 4637–4656 (2000).
46. Varga, G., Dagsson-Waldhauserová, P., Gresina, F. & Helgadottir, A. Saharan dust and giant quartz particle transport towards Iceland. *Sci. Rep.* **11**, 11891 (2021).
47. Israelevich, P., Ganor, E., Alpert, P., Kishcha, P. & Stupp, A. Predominant transport paths of Saharan dust over the Mediterranean Sea to Europe. *J. Geophys. Res.-Atmospheres* **117**, D02205 (2012).
48. Cuevas-Agulló, E. et al. Sharp increase in Saharan dust intrusions over the western Euro-Mediterranean in February–March 2020–2022 and associated atmospheric circulation. *Atmos. Chem. Phys.* **24**, 4083–4104 (2024).
49. Merz, N., Raible, C. C. & Woollings, T. North Atlantic eddy-driven jet in interglacial and glacial winter climates. *J. Climate* **28**, 3977–3997 (2015).
50. Roberts, W. H., Li, C. & Valdes, P. J. The mechanisms that determine the response of the Northern Hemisphere's stationary waves to North American ice sheets. *J. Climate* **32**, 3917–3940 (2019).
51. Wang, N., Jiang, D. & Lang, X. Northern westerlies during the Last Glacial Maximum: Results from CMIP5 simulations. *J. Climate* **31**, 1135–1153 (2018).
52. Kok, J. F. et al. Improved representation of the global dust cycle using observational constraints on dust properties and abundance. *Atmos. Chem. Phys.* **21**, 8127–8167 (2021).
53. Szopa, S. et al. Short-Lived Climate Forcers. in *Climate Change 2021: The Physical Science Basis. Contribution of Working Group I to the Sixth Assessment Report of the Intergovernmental Panel on Climate Change* (eds. Masson-Delmotte, V. et al.) 817–922 (Cambridge University Press, Cambridge, United Kingdom and New York, NY, USA, 2021). https://doi.org/10.1017/9781009157896.008.
54. Adebiyi, A. et al. A review of coarse mineral dust in the Earth system. *Aeolian Res* **60**, 100849 (2023).
55. Kok, J. F. et al. Mineral dust aerosol impacts on global climate and climate change. *Nature Rev. Earth Environ.* **1**, 16 (2023).
56. Legrand, M. et al. Alpine ice core record of large changes in dust, sea-salt, and biogenic aerosol over Europe during deglaciation. *PNAS Nexus* pgaf186 https://doi.org/10.1093/pnasnexus/pgaf186 (2025).
57. Albani, S. et al. Improved dust representation in the Community Atmosphere Model. *J. Adv. Model. Earth Syst.* **6**, 541–570 (2014).
58. Mahowald, N., Albani, S., Engelstaedter, S., Winckler, G. & Goman, M. Model insight into glacial-interglacial paleodust records. *Quat. Sci. Rev.* **30**, 832–854 (2011).
59. Lautridou, J. P., Sommé, J., Heim, J., Puisségur, J. J. & Rousseau, D. D. La stratigraphie des loess et formations fluviatiles d'Achenheim (Alsace): Nouvelles données bioclimatiques et corrélations avec les

séquences Pléistocènes de la France du Nord-Ouest. *Bull. Assoc. Fr. Etude Quat.* **22-23**, 125–132 (1985).
60. Antoine, P., Catt, J., Lautridou, J. P. & Somme, J. The loess and coversands of northern France and southern England. *J. Quat. Sci.* **18**, 309–318 (2003).
61. Antoine, P. et al. High-resolution record of the last interglacial-glacial cycle in the nussloch loess-palaeosol sequences, upper rhine area, Germany. *Quat. Int.* **76–77**, 211–229 (2001).
62. Rozycki, S. Z. Le sens des vents portant la poussière de loess à la lumière de l'analyse des formes d'accumulation du loess en Bulgarie et en Europe Centrale. *Rev. Geomorphol. Dyn.* **1**, 1–9 (1967).
63. Léger, M. Loess Landforms. *Quat. Int.* **7/8**, 53–61 (1990).
64. Chauvel, C., Bureau, S. & Poggi, C. Comprehensive Chemical and Isotopic Analyses of Basalt and Sediment Reference Materials. *Geostand. Geoanal. Res.* **35**, 125–143 (2011).
65. Hopcroft, P. O. & Valdes, P. J. On the role of dust-climate feedbacks during the mid-Holocene. *Geophys. Res. Lett.* **46**, 1612–1621 (2019).
66. Tindall, J. & Haywood, A. Modelling the mid-Pliocene warm period using HadGEM2. *Glob. Planet. Change* **186**, 103110 (2020).
67. Booth, B., Dunstone, N., Halloran, P., Andrews, T. & Bellouin, N. Aerosols implicated as a prime driver of twentieth-century North Atlantic climate variability. *Nature* **484**, 228–U110 (2012).
68. Caesar, J. et al. Response of the HadGEM2 Earth System Model to Future Greenhouse Gas Emissions Pathways to the Year 2300. *J. Climate* **26**, 3275–3284 (2013).
69. Woodward, S. *Mineral Dust in HadGEM2*. (Met Office, 2011).
70. Woodward, S. et al. The simulation of mineral dust in the United Kingdom Earth System Model UKESM1. *Atmos. Chem. Phys.* **22**, 14503–14528 (2022).
71. Bellouin, N. et al. The HadGEM2 family of met office unified model climate configurations. *Geosci. Model. Dev.* **4**, 723–757 (2011).
72. Fiedler, S. et al. A process-based evaluation of dust-emitting winds in the CMIP5 simulation of HadGEM2-ES. *Clim. Dyn.* **46**, 1107–1130 (2016).
73. Hopcroft, P. & Valdes, P. How well do simulated last glacial maximum tropical temperatures constrain equilibrium climate sensitivity?. *Geophys. Res. Lett.* **42**, 5533–5539 (2015).
74. Hopcroft, P., Valdes, P., O'Connor, F., Kaplan, J. & Beerling, D. Understanding the glacial methane cycle. *Nature Communications* **8**, 14383 (2017).
75. Peltier, W. R. Global glacial isostasy and the surface of the ice-age Earth: the ICE-5G (VM2) model and GRACE. *Annu. Rev. Earth Planet. Sci.* **32**, 111–149 (2004).
76. Petit, J.-R. et al. Climate and atmospheric history of the past 420,000 years from the Vostok ice core, Antarctica. *Nature* **399**, 429–436 (1999).
77. Spahni, R. et al. Atmospheric methane and nitrous oxide of the late Pleistocene from Antarctic ice cores. *Science* **310**, 1317–1321 (2005).
78. Loulergue, L. et al. Orbital and millennial-scale features of atmospheric CH4 over the past 800,000 years. *Nature* **453**, 383–386 (2008).
79. Berger, A. L. Long-term variations of caloric insolation resulting from the Earth's orbital elements. *Quat. Res.* **9**, 139–167 (1978).
80. Singarayer, J. S. & Valdes, P. J. High-latitude climate sensitivity to ice-sheet forcing over the last 120 kyr. *Quat. Sci. Rev.* **29**, 43–55 (2010).
81. Valdes, P. J. et al. The BRIDGE HadCM3 family of climate models: HadCM3@Bristol v1.0. *Geosci. Model. Dev.* **10**, 3715–3743 (2017).
82. Rousseau, D.-D. et al. Geochemical signature of last glacial maximum European loess samples [dataset bundled publication]. PANGAEA 10.1594/PANGAEA.971902 (2024).
83. Antoine, P. et al. High-resolution record of the environmental response to climatic variations during the Last Interglacial-Glacial cycle in Central Europe: The loess-palaeosol sequence of Dolní Věstonice (Czech Republic). *Quat. Sci. Rev.* **67**, 17–38 (2013).
84. Mellett, C. L. et al. Denudation of the continental shelf between Britain and France at the glacial-interglacial timescale. *Geomorphology* **203**, 79–96 (2013).
85. Rudnick, R. L. & Gao, S. 3.01-Composition of the continental crust. in *Treatise on Geochemistry* vol. 3 1–64 (Pergamon, Oxford, 2003).

Acknowledgements

We thank Peter Clark, Hubertus Fischer and Eric Wolff for their comments which greatly contributed to improving the draft. The authors thank three anonymous reviewers for their constructive comments that helped improve the quality of the manuscript. This project has been supported by the French LEFE-INSU national program through the IMAGO sub-program (D.-D.R.) and benefited of support from the IPGP multidisciplinary program PARI, by the Region Ile-de-France SESAME Grants no. 12015908 and EX047016 and by the IdEx Université de Paris grant ANR-18-IDEX0001. POH is supported by NERC (NE/X000567/1, NE/X000869/1 and NE/Z000025/1) and the Birmingham Environment for Academic Research (BEAR high-performance computing, http://www.bear.bham.ac.uk).

Author contributions

Conceptualization: D.-D.R. Investigation: D.-D.R., C.C., P.H. Methodology: all authors - D.-D.R., C.C, P.H., P.G., S. S.-C., P.A., M. F., A;U. Writing - original draft: D.-D.R., C.C., P.H. with initial comments from P.A. and M. F. Writing -review and editing: D.-D.R., C.C., P.H.

Competing interests

The authors declare no competing interests.

Additional information

Supplementary information The online version contains supplementary material available at https://doi.org/10.1038/s43247-025-02888-9.

Correspondence and requests for materials should be addressed to Denis-Didier Rousseau.

Peer review information *Communications Earth and Environment* thanks the anonymous reviewers for their contribution to the peer review of this work. Primary Handling Editors: Carolina Ortiz Guerrero and Mengjie Wang. A peer review file is available.